Journal of Power Sources 317 (2016) 19–24

Contents lists available at ScienceDirect

Journal of Power Sources

journal homepage: www.elsevier.com/locate/jpowsour

Prism-patterned Nafion membrane for enhanced water transport in polymer electrolyte membrane fuel cell

Sang Moon Kim [a, b, 1], Yun Sik Kang [c, 1], Chiyeong Ahn [d, e], Segeun Jang [b, f], Minhyoung Kim [d, e], Yung-Eun Sung [d, e], Sung Jong Yoo [c, *], Mansoo Choi [b, f, **]

[a] Department of Mechanical Engineering, Incheon National University, Incheon, 406-772, Republic of Korea
[b] Global Frontier Center for Multiscale Energy Systems, Seoul National University, Seoul 151-744, Republic of Korea
[c] Fuel Cell Research Center, Korea Institute of Science and Technology (KIST), Seoul 136-791, Republic of Korea
[d] Center for Nanoparticle Research, Institute for Basic Science (IBS), Seoul 151-742, Republic of Korea
[e] School of Chemical and Biological Engineering, Seoul National University, Seoul 151-742, Republic of Korea
[f] Division of WCU Multiscale Mechanical Design, Department of Mechanical and Aerospace Engineering, Seoul National University, Seoul, 151-742, Republic of Korea

HIGHLIGHTS

- A prism-patterned Nafion membrane was used in membrane electrode assembly (MEA).
- The MEA exhibited improved performance especially at high current density.
- Asymmetric geometry of the prism structure facilitated water removal from cathode.

ARTICLE INFO

Article history:
Received 11 January 2016
Received in revised form
4 March 2016
Accepted 24 March 2016

Keywords:
Polymer electrolyte membrane fuel cell
Prism array
Asymmetric geometry
Reduced membrane resistance
Enhanced water transport

ABSTRACT

Here, we report a simple and effective strategy to enhance the performance of the polymer electrolyte membrane fuel cell by imprinting prism-patterned arrays onto the Nafion membrane, which provides three combined effects directly related to the device performance. First, a locally thinned membrane via imprinted micro prism-structures lead to reduced membrane resistance, which is confirmed by electrochemical impedance spectroscopy. Second, increments of the geometrical surface area of the prism-patterned Nafion membrane compared to a flat membrane result in the increase in the electrochemical active surface area. Third, the vertically asymmetric geometry of prism structures in the cathode catalyst layer lead to enhanced water transport, which is confirmed by oxygen gain calculation. To explain the enhanced water transport, we propose a simple theoretical model on removal of water droplets existing in the asymmetric catalyst layer. These three combined effects achieved via incorporating prism patterned arrays into the Nafion membrane effectively enhance the performance of the polymer electrolyte membrane fuel cell.

1. Introduction

As an eco-friendly alternative energy device, the polymer electrolyte membrane fuel cell (PEMFC) has received much positive attention in the aspect of high energy conversion efficiency without generating pollutant emissions such as CO_2, NO_x and SO_x [1–3]. However, there have been many practical issues related to the commercialization of PEMFC such as slow electrochemical reaction of Pt catalyst with oxygen at the cathode, so called oxygen reduction reaction (ORR) [4,5], catalyst poisoning by carbon monoxide [6–8], water management in the membrane electrode assembly (MEA) [9–11] and so forth. Of all these issues, water management at the cathode is one of the most crucial issues for enhancing overall cell performance, because the water produced from cell reaction impedes the oxygen transport into the triple-phase boundary in the cathode catalyst layer and then the significant

* Corresponding author.
** Corresponding author. Global Frontier Center for Multiscale Energy Systems, Seoul National University, Seoul 151-744, Republic of Korea.
E-mail addresses: ysj@kist.re.kr (S.J. Yoo), mchoi@snu.ac.kr (M. Choi).
[1] These authors contributed equally to this work.

http://dx.doi.org/10.1016/j.jpowsour.2016.03.083
0378-7753/

cell voltage drop takes place in sequence if it is not properly removed from the cathode [1,10–12].

For previous decades, numerous researches related to water management at the cathode have been conducted such as hydrophobic surface treatment and structural modification of the cathode catalyst layer by using the pore formers including carbonate particles or polystyrene (PS) beads [13–15]. In spite of these efforts, the water management issue has not been thoroughly resolved due to technical issues including sharp decrease in the electrochemical active surface area (ECSA) of the catalyst layer [16,17] and thickened MEA with lower mechanical robustness that bears the detrimental effect on the long term stability of MEAs [13,15].

To address these issues, a simple and effective method for enhanced water management at the cathode in PEMFC is highly required. In this paper, we introduce the method for improving water management by using a prism-patterned Nafion membrane as a polymer electrolyte in MEA. This MEA with the prism-patterned Nafion membrane exhibited improved performance especially at a high current density because the water produced at the cathode was easily removed via the asymmetric geometry of the prism structure in the catalyst layer. Furthermore, performance enhancement via reduced membrane resistance and increased electrochemical active surface area was achieved with the patterned MEA.

2. Experimental

2.1. Preparation of the prism patterned Nafion membrane

The prism array masters used in the present study were prepared mechanically. First, a blank roll or plate of stainless steel electroplated by nickel was prepared. The blank roll or plate surface was machined by a diamond-cutting tool with a specific angle. In this process, the height of the patterns depends on the cutting depth of the diamond tool. In this study, a prism master with 50 μm in period and 45° in prism angle was used. After the preparation of the master, a mixture of base and curing agent (10: 1 w/w) of Sylgard 184 PDMS elastomer was poured onto the patterned masters and cured at 70 °C for 2 h. The cured PDMS molds were peeled off from the master and cut prior to use. Then, PFPE (Perfluoropolyether) prism mold was fabricated via UV replica molding by using the PDMS prism mold. Then, the Nafion 212 membrane (Dupont) was uniformly placed between an as-prepared PFPE mold and glass substrate. Then, the sandwiched assembly was imprinted under hydraulic pressure (10–20 kg cm^{-2}) and temperature (~95 °C) for 10 min. After cooled down to room temperature, the patterned Nafion membrane was peeled off from the PFPE mold and kept in a deionized water container for approximately 12 h.

2.2. Physical analysis

Field emission-scanning electron microscopy (FE-SEM) was conducted using a SUPRA 55VP microscope (Carl Zeiss) to measure the morphology of the various samples used in this paper.

2.3. Preparation of MEAs

The catalyst ink was prepared by mixing water, 5 wt% Nafion solution (DuPont) and isopropyl alcohol (IPA) (Aldrich) with the catalyst. 40 wt% Pt/C (Johnson Matthey) was used for the anode and cathode catalyst inks, respectively. The prepared catalyst ink was blended by the ultrasonic treatment and sprayed onto the anode and cathode sides of the bare Nafion 212 membrane and prism-patterned Nafion membrane to fabricate MEAs. The Pt catalyst loadings were equally 0.12 mg cm^{-2} in the anodes and cathodes of the MEAs according to DOE conditions [18,19]. These catalyst-coated membranes (CCMs) were dried at room temperature for more than 12 h, and sandwiched between the anode and cathode gas diffusion layers (GDLs, SGL 35 BC) without a hot-press process. The active geometric areas of the MEAs were 5.0 cm^2.

2.4. Electrochemical measurements

For the single cell performance test at 80 °C, humidified H_2 and O_2 (air) gases were flowed into the anode and cathode, respectively. The stoichiometric coefficient of H_2/O_2 (air) was 2.0/9.5 (2.0) under the ambient pressure. Additionally, the relative humidities (RHs) for the anode and cathode gases were 100%. Electrochemical impedance spectroscopy (EIS) (IM6, Zahner) of the single cells was measured at 0.6 V with an amplitude of 5 mV. The measurement was conducted in the frequency range from 0.1 Hz to 100 kHz. Other experimental conditions, such as temperature and gas humidification, were the same as for the single-cell operation at 80 °C with H_2/Air. The ZView program (Scribner Associates Inc.) was used to fit the EIS data, and a simple equivalent circuit was applied. Cyclic voltammograms (CVs) were obtained at 100 mV s^{-1} between 0.05 and 1.20 V to measure the electrochemical active surface area (ECSA) of the prepared cathode catalyst layers at room temperature. Humidified H_2 and N_2 gases were supplied to the anode and cathode, respectively, and RHs were 100%. The anode with H_2 gas flowing around was used as the reference and counter electrodes, and the cathode with N_2 gas served as a working electrode.

3. Results and discussion

The procedure for the fabrication of MEA with the prism-patterned Nafion membrane is illustrated in Fig. 1. First, the prism-patterned Nafion membrane was prepared by imprinting 50 μm-period prism-patterned architectures into a bare Nafion 212 membrane under hydraulic pressure and temperature. To figure out the swelling effect of the prism patterns of Nafion membrane, we observed the cross-sectional images before and after swelling by absorbed water [20,21]. As shown in Fig. S1, the geometrical features including thickness and patterned-shape of the Nafion membrane are comparable before and after swelling. And the prism patterned Nafion membrane exhibits the same level of stress distribution of Nafion 212 (thickness ~ 50 μm) in the simulation study when the same stress applied to the membrane, which indicates the sufficient mechanical stability even with the locally thinned layer of the prism patterned Nafion membrane as shown in Fig. S2. In the following step, Pt/C catalysts were air-sprayed onto both sides of the prism-patterned Nafion membrane to fabricate catalyst layers for MEA (Pt catalyst loading: 0.12 mg cm^{-2}). The corresponding SEM images of the prism mold, imprinted Nafion membrane and catalyst-coated Nafion membrane at the cathode side clearly displayed prism-patterned architectures, which indicate that the materials and the preparation step used for the fabrication of MEA with the prism-patterned Nafion membrane were sufficient and suitable. In addition, it was clearly shown that Pt/C catalyst layer was fabricated following the structure of the prism-patterned Nafion.

The prepared MEA with the prism-patterned Nafion membrane was operated in a fully humidified condition of H_2/O_2 (H_2/air) and exhibited highly improved performance under all conditions compared with the conventional one, expressed in Fig. 2. Especially, the MEA with the prism-patterned Nafion membrane exhibited the maximum power density of 0.72 W cm^{-2} in the case of H_2/air conditions, which is higher than that of the conventional one (0.48 W cm^{-2}) by 50% (Table S1).

These performance enhancements can be explained by the

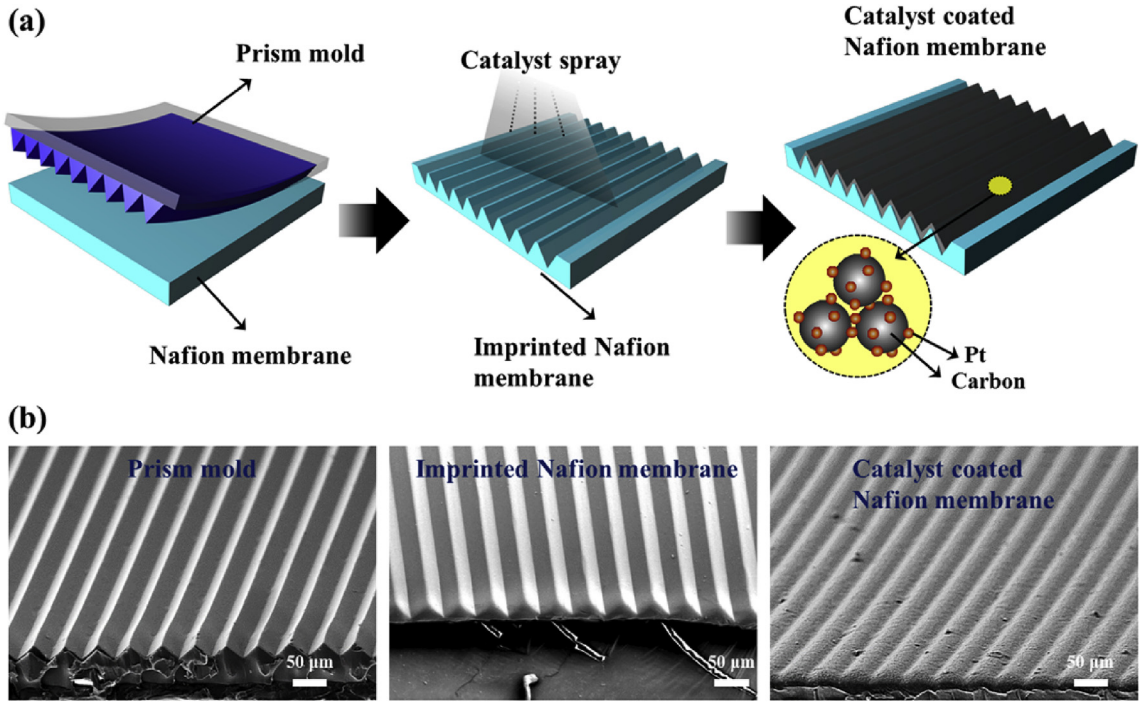

Fig. 1. (a) Schematic illustration of imprinting prism-patterned array onto Nafion membrane and constructing membrane electrode assembly (MEA) by Pt/C catalysts spraying process. (b) Corresponding SEM images of PFPE (Perfluoropolyether) prism mold, imprinted Nafion membrane and catalyst coated membrane (CCM) from the left side.

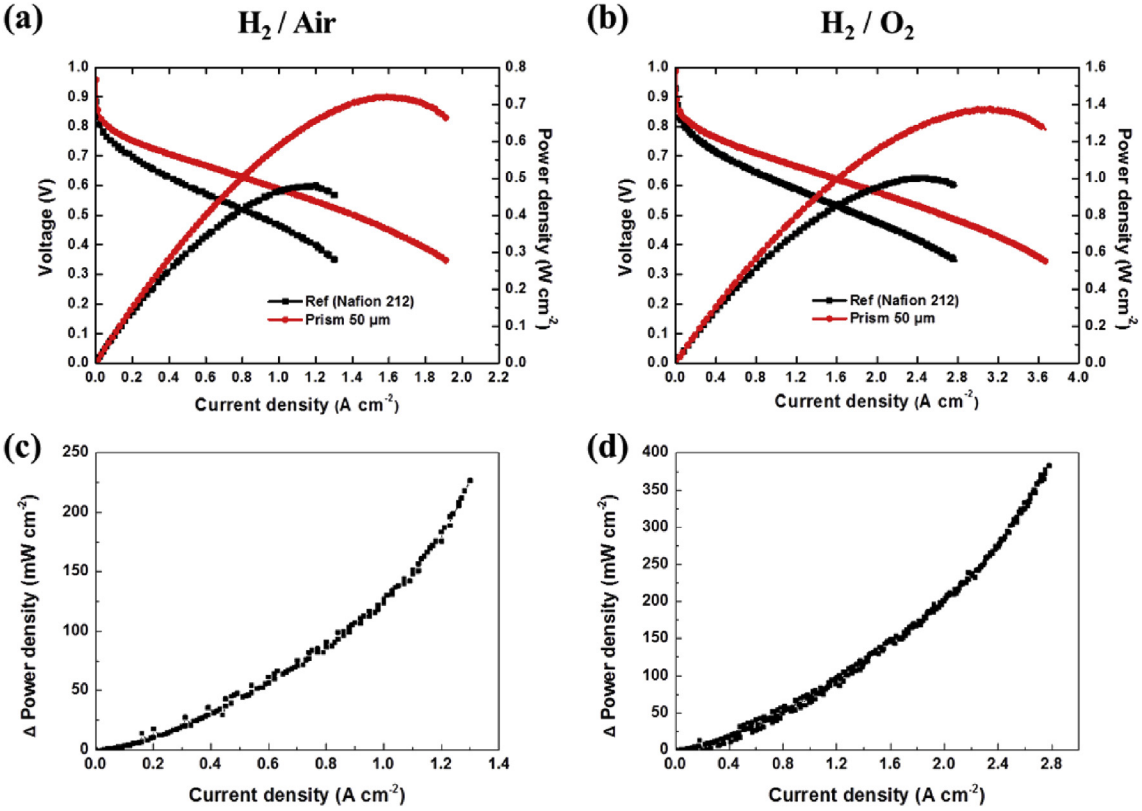

Fig. 2. (a) Polarization curves of conventional membrane electrode assembly (MEA) and the MEA with the prism patterned Nafion membrane under the conditions of H_2/Air (a) and H_2/O_2 (b). The graphs for differences of power density between conventional MEA and prism patterned MEA under the conditions of H_2/Air (c) and H_2/O_2 (d).

effects from the geometrical feature of the prism pattern. First, as previously studied, reduced membrane thickness by imprinting prism patterns lowered ohmic resistance during the PEMFC operation [18]. Second, water transport enhancement which was

confirmed by increased difference of power density with increasing current density contributed to the performance enhancement as shown in Fig. 2c and d. The geometrical feature of the prism pattern is triangular in a cross sectional view, which is asymmetric feature. This characteristic may contribute to the enhancement of water transport. Additional electrochemical experiments were conducted to elucidate the performance enhancement by the effects resulted from the geometrical feature of the prism pattern. Furthermore, it is also expected that the enlarged electrochemically active area by the increment of the geometrical surface area of the Nafion membrane has a minor contribution to the performance enhancement [18,22].

At first, the asymmetric geometry of the prism structure in the cathode catalyst layer for enhanced water transport at the cathode was evaluated by using oxygen gain. The oxygen gain was obtained by calculating potential difference when oxygen and air are supplied respectively [13,23] over given current density range. Using the oxygen gain, the degree of mass transfer at the cathode catalyst layer was confirmed. In Fig. 3a, the calculated oxygen gain of the MEA with the prism-patterned Nafion membrane exhibited much lower values than that of the conventional one, which means that the asymmetric geometry of prism structures in the cathode catalyst layer removes produced water much more easily and supplies fuel gas more effectively than the conventional one. Hence, due to the asymmetric structure of the cathode catalyst layer, MEA with the prism-patterned Nafion membrane exhibited improved performance than the conventional one, especially at high current density. To further investigate the improved water transport effect, we additionally conducted performance measurements under the outlet pressure of 150 kPa. With the additional pressure, gas diffusion would be more facilitated than ambient pressure condition and the utilization of Pt catalyst at each electrode would be maximized [19,24–26], therefore, we can confirm the mass transport effect more directly. Fig. S3 shows that the difference between the power densities of MEAs with prism patterned Nafion membrane and conventional one was rapidly increased in the high current region above ~0.8 A cm^{-2}, at which the cells began to be severely affected by mass transport in the MEAs. However, the difference in the low current region below ~0.8 A cm^{-2} was not shown because those current densities were mainly governed by the charge transport without flooding in the cathodes.

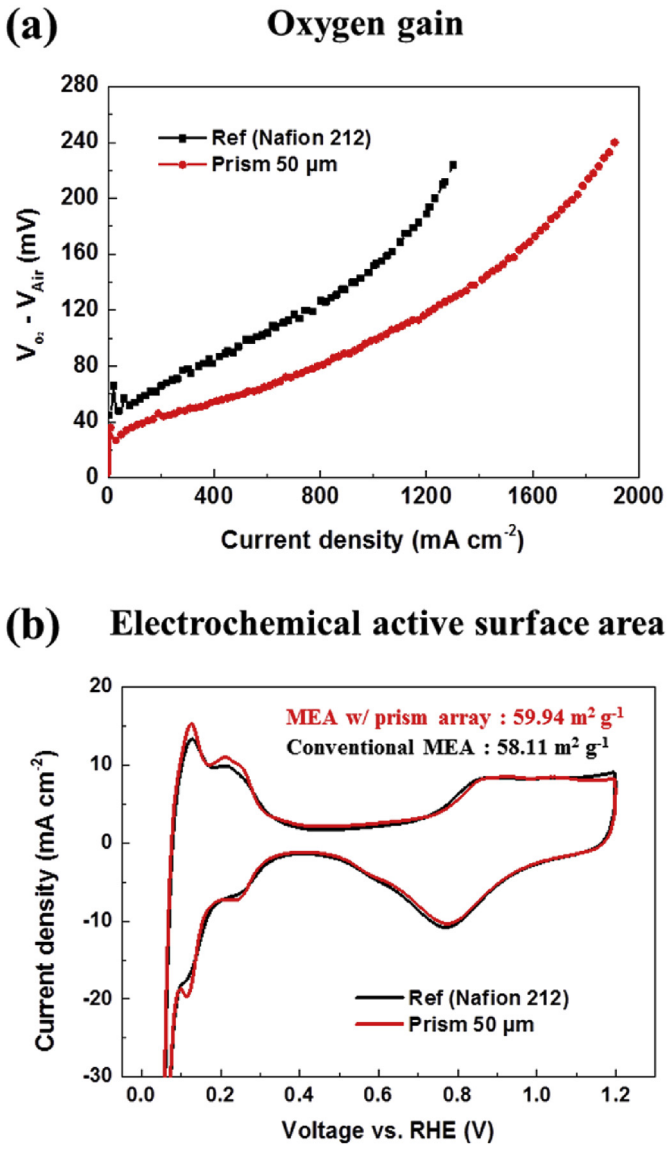

Fig. 3. (a) The graph for the oxygen gain obtained by calculating potential difference when oxygen and air are supplied respectively. (b) Cyclic voltammogram (CV) of the cathode catalyst layers of the conventional MEA and the prism patterned MEA.

In addition, to quantitatively investigate the effect of increased electrochemical active surface area (ECSA) and reduced ohmic resistance, both cyclic voltammetry (CV) [27] and electrochemical impedance spectroscopy (EIS) [28–30] test were conducted. As shown in Fig. 3b, the ECSA for our patterned membrane (59.94 cm^2 g^{-1}) was slightly larger compared with that of the reference cell (58.11 cm^2 g^{-1}), which resulted from the increment of the geometrical surface area (1.41-fold than the surface area of the flat one). Next, EIS data were obtained at 0.6 V vs. RHE under H_2/air conditions and were fitted by using PEMFC equivalent circuit (L_W = inductance of the electric wire, $R_{membrane}$ = internal membrane resistance, $R_{cathode\ (anode)}$ = charge transfer resistance of the cathode (anode), $CPE_{cathode\ (anode)}$ = constant phase element of the cathode (anode) and Z_W = Warburg impedance) (Fig. 4a, b and Table S2). From the fitted data, we found relatively lower features, in the case of the constructed MEA (in situ) with the prism-patterned Nafion membrane than the conventional one: ohmic resistance ($R_{membrane}$) by ~22.4%, charge transfer resistance at the cathode ($R_{cathode}$) by ~27.3% and Warburg impedance (Z_w) by ~33.2% without big differences from anode ones (Table S2). It is concluded that i) reduced membrane thickness by imprinting lowered $R_{membrane}$ values considerably, ii) enlarged ECSA and facilitated water removal from the cathode catalyst layer by the effect of the asymmetric geometry of the prism structure and, as a result, improved cathode reaction and better oxygen supply reduced R_{ct} and Z_w values significantly. Therefore, increased ECSA and decreased cell resistance for our prism-patterned case can explain the increase in maximum power density of MEA with the prism-patterned Nafion membrane.

To address the issue of durability of the MEA with the prism-patterned Nafion membrane, we performed accelerated durability test (ADT), which were conducted by using CV method in the potential range of 0.05–1.20 V vs. RHE and 100 mV s^{-1} at RT for 5000 cycles with fully humidified H_2/N_2 gases supplied to anode and cathode, respectively [31]. After ADT, performances of both MEAs with flat and prism-patterned Nafion membrane decreased as shown in Fig. S4, resulted from the degradation of Pt electrocatalyst and increased interfacial resistance between the Nafion membrane and the cathode catalyst layer as depicted in Fig. S5. However, even after ADT tests, the performance of MEA with prism-patterned Nafion membrane was still higher than MEA with flat membrane by ~23.8% (~35.1%) of maximum power density in the case of H_2/O_2 (air) conditions under ambient pressure, especially in high current

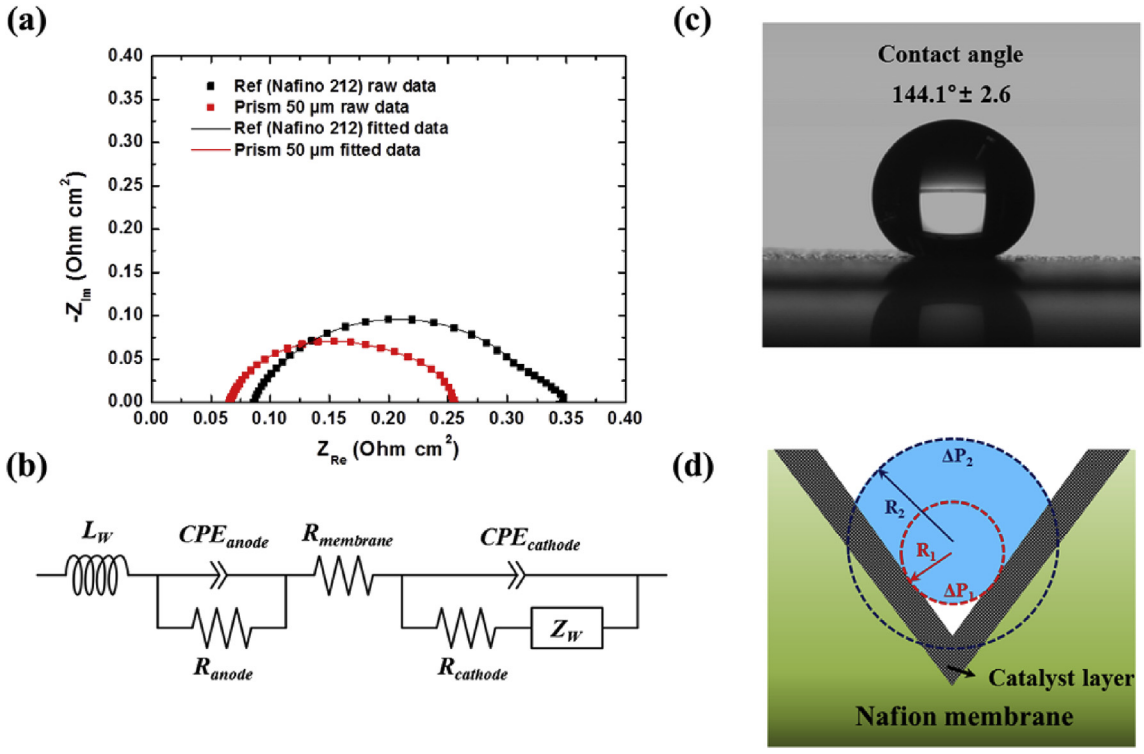

Fig. 4. (a) Electrochemical impedance spectroscopy (EIS) of the conventional MEA and the prism patterned MEA at 0.6 V compared with RHE. (b) Equivalent circuit of the PEMFC. (c) The contact angle of a DI water droplet on the cathode catalyst layer of the conventional MEA. (d) Schematic illustration for a water droplet at a void space in the catalyst layer which has different curvatures in the top side and bottom side.

density region. The result showed that the improved water transport effect by the prism structure of membrane maintained even after the test.

To understand the enhanced water transport in the catalyst layer with the vertically asymmetric prism structure, we propose a simple theoretical model termed an asymmetric channel system. We hypothesize that the water was transported from the catalyst layer to the GDL layer in the form of a droplet. The contact angle of the water droplet on the catalyst layer of conventional MEA was ~144.1° (±2.6), which means that the catalyst layer was almost superhydrophobic [10] as shown in Fig. 4c, hence, the water generated from electrochemical reaction was easily dewetted from the surface of the catalyst layer. Therefore, water could exist as a droplet at a void space in the catalyst layer as shown in Fig. 4d. Then, the droplet had different curvatures in the top side and the bottom side with forming the asymmetric shape. The pressure difference between the inside and outside of the droplet, Laplace pressure, can be calculated from the well-known Laplace-Young equation [32,33]:

$$\Delta P = P_{inside} - P_{outside} = 2\gamma/R \quad (1)$$

where γ is the surface tension and R is the radius of curvature of the water droplet. The asymmetric shape of the droplet means that there are Laplace pressures difference between the top side and bottom side of the droplet [33,34]. As shown in Fig. 4d, the bottom side of the droplet has larger curvature, which means higher Laplace pressure than the top side of the droplet. And the Laplace pressures difference induces the droplet to move upward easily with the aid of the geometrical feature of the prism shaped electrode [35–37].

4. Conclusions

In summary, we proposed a novel method for improving water management by using a prism-patterned Nafion membrane as a polymer electrolyte for MEA. MEA with the prism-patterned Nafion membrane exhibited improved performance especially at high current density than the conventional one, because of the asymmetric geometry of the prism structure in the cathode catalyst layer, which removes produced water much easily and supplies fuel gas more effectively by the Laplace pressure difference. Furthermore, performance enhancement via reduced membrane resistance and increased electrochemical active surface area was achieved for the MEA with the prism-patterned Nafion membrane. Our novel approach of the use of asymmetric structures surely possesses potential to be applied to other energy conversion and storage devices.

Acknowledgments

This work was supported by the Global Frontier R&D Program of the Center for Multiscale Energy Systems and funded by the National Research Foundation under the Ministry of Science, ICT&Future Planning (under contracts No. NRF-2011-0031561, NRF-2012M3A6A7054283), the NRF grant funded by MSIP (2014R-1A2A2A04003865), and the KETEP granted financial resource from MOTIE (20143010031840), Korea.

Appendix A. Supplementary data

Supplementary data related to this article can be found at http://dx.doi.org/10.1016/j.jpowsour.2016.03.083.

References

[1] H.A. Gasteiger, N.M. Marković, Science 324 (2009) 48–49.
[2] R.P. O'Hayre, S.-W. Cha, W. Colella, F.B. Prinz, Fuel Cell Fundamentals, John Wiley & Sons New York, 2006.
[3] F. Barbir, PEM Fuel Cells, Springer, 2006.
[4] I.E.L. Stephens, A.S. Bondarenko, U. Grønbjerg, J. Rossmeisl, I. Chorkendorff, Energy Environ. Sci. 5 (2012) 6744–6762.
[5] P. Costamagna, S. Srinivasan, J. Power Sources 102 (2001) 242–252.
[6] D. Wang, C.V. Subban, H. Wang, E. Rus, F.J. DiSalvo, H.D. Abruña, J. Am. Chem. Soc. 132 (2010) 10218–10220.
[7] J. Baschuk, X. Li, Int. J. Energy Res. 25 (2001) 695–713.
[8] Z. Qi, C. He, A. Kaufman, J. Power Sources 111 (2002) 239–247.
[9] P.K. Sinha, P.P. Mukherjee, C.Y. Wang, J. Mater. Chem. 17 (2007) 3089–3103.
[10] N. Jung, S.M. Kim, D.H. Kang, D.Y. Chung, Y.S. Kang, Y.-H. Chung, Y.W. Choi, C. Pang, K.-Y. Suh, Y.-E. Sung, Chem. Mater 25 (2013) 1526–1532.
[11] H. Li, Y. Tang, Z. Wang, Z. Shi, S. Wu, D. Song, J. Zhang, K. Fatih, H. Wang, J. Power Sources 178 (2008) 103–117.
[12] P.P. Mukherjee, Q. Kang, C.Y. Wang, Energy Environ. Sci. 4 (2011) 346–369.
[13] Y.-H. Cho, N. Jung, Y.S. Kang, D.Y. Chung, J.W. Lim, H. Choe, Y.-H. Cho, Y.-E. Sung, Int. J. Hydrogen. Energ 37 (2012) 11969–11974.
[14] T.V. Reshetenko, H.-T. Kim, H.-J. Kweon, J. Power Sources 171 (2007) 433–440.
[15] J. Zhao, X. He, L. Wang, J. Tian, C. Wan, C. Jiang, Int. J. Hydrogen. Energ 32 (2007) 380–384.
[16] R. Friedmann, T. Van Nguyen, J. Electrochem. Soc. 157 (2010) B260–B265.
[17] X. Zhang, P. Shi, Electrochem. Commun. 8 (2006) 1229–1234.
[18] H. Cho, S.M. Kim, Y.S. Kang, J. Kim, S. Jang, M. Kim, H. Park, J.W. Bang, S. Seo, K.-Y. Suh, Nat. Commun. 6 (2015).
[19] O.-H. Kim, Y.-H. Cho, S.H. Kang, H.-Y. Park, M. Kim, J.W. Lim, D.Y. Chung, M.J. Lee, H. Choe, Y.-E. Sung, Nat. Commun. 4 (2013).
[20] P. Majsztrik, A. Bocarsly, J. Benziger, J. Phys. Chem. C 112 (2008) 16280–16289.
[21] S. Goswami, S. Klaus, J. Benziger, Langmuir 24 (2008) 8627–8633.
[22] J.K. Koh, Y. Jeon, Y.I. Cho, J.H. Kim, Y.-G. Shul, J. Mater. Chem. A 2 (2014) 8652–8659.
[23] M. Prasanna, H.Y. Ha, E. Cho, S.-A. Hong, I.-H. Oh, J. Power Sources 137 (2004) 1–8.
[24] A. Omosebi, R.S. Besser, J. Power Sources 228 (2013) 151–158.
[25] M. Amirinejad, S. Rowshanzamir, M.H. Eikani, J. Power Sources 161 (2006) 872–875.
[26] H.-N. Su, S.-J. Liao, T. Shu, H.-L. Gao, J. Power Sources 195 (2010) 756–761.
[27] S. Gouws, Voltammetric Characterization Methods for the PEM Evaluation of Catalysts, INTECH Open Access Publisher, 2012.
[28] X. Yuan, H. Wang, J.C. Sun, J. Zhang, Int. J. Hydrogen. Energ 32 (2007) 4365–4380.
[29] S.M.R. Niya, M. Hoorfar, J. Power Sources 240 (2013) 281–293.
[30] A. Kulikovsky, J. Electrochem. Soc. 162 (2015) F217–F222.
[31] X.-Z. Yuan, H. Li, S. Zhang, J. Martin, H. Wang, J. Power Sources 196 (2011) 9107–9116.
[32] G.M. Walker, D.J. Beebe, Lab. Chip 2 (2002) 131–134.
[33] M. Prakash, D. Quéré, J.W. Bush, Science 320 (2008) 931–934.
[34] Y. Zheng, H. Bai, Z. Huang, X. Tian, F.-Q. Nie, Y. Zhao, J. Zhai, L. Jiang, Nature 463 (2010) 640–643.
[35] J. Zhu, Y. Luo, J. Tian, J. Li, X. Gao, ACS Appl. Mater. Interfaces 7 (2015) 10660–10665.
[36] Y. Zheng, D. Han, J. Zhai, L. Jiang, Appl. Phys. Lett. 92 (2008) 084106.
[37] X. Chen, J. Wu, R. Ma, M. Hua, N. Koratkar, S. Yao, Z. Wang, Adv. Funct. Mater 21 (2011) 4617–4623.